



m-DOPA addition in MAPLE immobilization of lipase for biosensor applications



Valeria Califano^a, Giovanni Ausanio^{b,c}, Francesco Bloisi^{b,c}, Antonio Aronne^d,
Luciano R.M. Vicari^{b,c}, Libera Nasti^{e,*}

^a Istituto Motori – CNR, Napoli, Italy

^b Department of Physics, University of Naples “Federico II”, Napoli, Italy

^c SPIN – CNR, Napoli, Italy

^d Department of Chemical Engineering, Materials and Industrial Production, University of Naples “Federico II”, Napoli, Italy

^e Accademia di Belle Arti, Napoli, Italy

ARTICLE INFO

Article history:

Received 7 May 2015

Received in revised form 23 July 2015

Accepted 27 July 2015

Keywords:

MAPLE

Lipase

m-DOPA

Biosensors

ABSTRACT

Matrix Assisted Pulsed Laser Evaporation (MAPLE) is a thin film deposition technique which uses a pulsed laser beam impinging, inside a high vacuum chamber, on a frozen target containing the guest molecules in a volatile matrix to induce fast “evaporation” of the matrix, and ejection of the guest molecules. Lipase, an enzyme acting as a catalyst in hydrolysis of lipids, is widely used in biosensors for detection of triglycerides in blood serum. A key action to this purpose is lipase immobilization on a substrate. In a recent paper, we have shown that MAPLE technique is able to deposit lipase on a substrate in an active form. Here we show that addition to the guest/matrix target of a small amount of m-DOPA (3-(3,4-dihydroxyphenyl)-2-methyl-L-alanine) in order to improve adhesion and protect lipase secondary structure, also allows the lowering the laser pulse energy required for matrix evaporation and therefore the risk of damaging the enzyme.

© 2015 The Authors. Published by Elsevier B.V. This is an open access article under the CC BY-NC-ND license (<http://creativecommons.org/licenses/by-nc-nd/4.0/>).

1. Introduction

In Pulsed Laser Deposition (PLD), a pulsed laser beam impinging on a target made by the material to be deposited generates a plasma plume thus transferring molecules to the substrate placed in front of the target. This technique, widely used for deposition of high quality thin films [1], cannot be used for biological molecules, polymers, or other large and delicate molecules [2] that can be damaged by laser radiation. In order to avoid such damages the Matrix Assisted Pulsed Laser Evaporation (MAPLE) [3] technique uses a frozen target containing the molecules to be deposited (guest) in a volatile solvent (matrix) [4]. The pulsed laser beam impinging onto the frozen target causes an abrupt evaporation of the matrix containing the guest molecules. In the vacuum deposition chamber, the vacuum pump system takes away the volatile matrix molecules and only the guest molecules reach the substrate placed in front of the target. Details of our deposition system have been presented elsewhere [5]. Here we underline that the presence of the matrix avoids, or at least greatly reduces, laser induced damages to guest molecules. MAPLE deposition of polymers [6–10] or organic molecules such as proteins and enzymes [11–14] have been reported for several applications.

The sensing element in a biosensor usually combines an electrochemical probe with an appropriate enzyme thin layer [15,16]. In triglycerides (TG) biosensors [17–19], a usual choice for the enzyme is lipase since its chemical action is to catalyze the hydrolysis of triacylglycerol to glycerol and fatty acids.

TG biosensors are commonly obtained as Ion Sensitive Field Effect Transistors (ISFET) or as Electrolyte Insulator Semiconductor Capacitor (EISCAP) devices. The enzyme for hydrolysis must be immobilized in both cases on the sensor silicon substrate.

Today lipase immobilization still appears as a rather difficult task even if several techniques (physical adsorption onto an insoluble carrier [20], entrapment within a matrix [21], cross-linking [22] and covalent bonding [23] to an insoluble support) have been applied. Physical adsorption onto insoluble carriers is the most widespread way to immobilize lipases. It is carried out by dipping the support in a concentrated solution of lipase, allowing physical interactions between the enzyme and the carrier’s surface (Van der Waals forces, hydrogen bonding and hydrophobic interactions, etc.). This procedure presents the advantage of not involving chemical modification of the enzyme. On the other hand, several parameters, as the pH at which the adsorption is performed, affect the adsorption of lipase onto the carrier. Moreover, the adsorption of proteins on solid surfaces can induce structural changes that can affect the entire macromolecule and consequently its catalytic activity. Finally, the nature of the support is very important in determining the efficiency of the immobilization, as it can influence the

* Corresponding author.

conformation of the enzyme during adsorption. Most lipases show an increase in catalytic activity when they are immobilized on hydrophobic surfaces. This is associated to conformational changes in the enzyme upon adsorption, creating an open, substrate-accessible active site. This means that lipases recognize hydrophobic surfaces similar to those of their natural substrates and they undergo interfacial activation during immobilization [24].

The ability to preserve the native conformation of the enzyme hence influences the immobilization efficiency.

In a recent work [25], we have shown that it is possible, using MAPLE technique, to deposit lipase on a substrate partially preserving its conformational characteristics.

Mussel fouling on a variety of wet surfaces is due to the secretion of liquid Mussel Protein Adhesives (MAP) that rapidly harden to form a solid adhesive plaque capable of granting good adhesion to a wide variety of wet surfaces [26–29].

MeFP-1 (*Mytilus edulis* Foot Protein 1) contains 15% of L-DOPA (3,4-dihydroxy-phenyl-L-alanine), responsible for the adhesive and cohesive properties of mussel adhesive proteins. The cohesive role derives from reactions following the oxidation of DOPA to DOPA-quinone, while unoxidized DOPA has an adhesive action. Similar properties can be found in m-DOPA (3-(3,4-dihydroxyphenyl)-2-methyl-L-alanine), an analogous of L-DOPA with a methyl group added in order to improve its solubility in water. In a previous paper [30] we have discussed and demonstrated the use of MAPLE deposition of m-DOPA in improving PEG adhesion for anti-biofouling applications.

Here, we report the MAPLE deposition of lipase adding m-DOPA as an excipient to protect lipase from denaturation induced by freezing and drying during plume expansion [31]. Moreover, m-DOPA absorbs the infrared laser radiation used, since around 1064 nm there is the third overtone of C–H stretching of aromatic groups [32], while water does not have absorption bands near that wavelength.

2. Materials and methods

Candida Rugosa Lipase (CRL) type VII, obtained by Sigma–Aldrich, was chosen for its positional aspecificity, i.e. the ability of acting on all glyceride bonds, not depending on their position. Non-buffered demineralized water was used as solvent. Target solution was prepared by dissolving the appropriate quantity of lipase in water (sample M-L1) and adding the right quantity of an m-DOPA aqueous solution (samples M-L2 and M-L3). The required amount of m-DOPA was added as a 1.0 wt% suspension in bi-distilled water starting from an m-DOPA hemihydrate powder (obtained from Fluka).

About 2 mL of freshly prepared matrix/guest solution was placed in the target holder inside the vacuum chamber and the target was frozen by placing it in thermal contact with liquid nitrogen contained in a reservoir connected to the MAPLE deposition system. The target temperature was lowered to about -130 °C and kept at this value during the whole deposition procedure.

The vacuum chamber pressure was lowered, after target freezing, to about 10^{-4} Pa, but its values increased by about one order of magnitude during deposition due to the presence of matrix vapor generated by laser pulses.

The substrate was placed in front of the target at a distance of about 0.9 cm. Such unusually short target to substrate distance was chosen to maximize the deposition yield for sample characterization, since here we are focused on the deposition of undamaged lipase rather than on the optimization of the film morphology. The Nd:YAG pulsed laser was operated at its fundamental wavelength (1064 nm). Even if the Q-switched Nd:YAG laser can be also operated at wavelengths corresponding to second, third or fourth harmonics (532 nm, 355 nm, 266 nm respectively), the IR laser wavelength was chosen in order to minimize photochemical damage of lipase, since it has a large absorption band [33], centered at 280 nm, in the UV region mainly used for MAPLE deposition.

The laser beam reached the target at an angle of 45°, partially focused to an ellipsoidal area of about 1.0 mm by 1.4 mm. The target was moved back and forth by a computerized 2D translation system so that, in order to avoid drilling, the beam scanned (one or more times, depending on the total number of pulses) a target area of about 1.5 cm². The values of the parameters of the laser beam (pulse repetition rate: 4 pulses per second, energy pulse: see Table 1, and number of pulses: 29720) have been discussed elsewhere [5]. Target composition for each sample is shown in Table 1 together with the lowest pulse energy required to get a MAPLE deposition. In order to facilitate subsequent FTIR analysis of the samples, 13 mm diameter KBr pellets were chosen as substrates for MAPLE deposition.

FTIR spectra were recorded, in the 4000–400 cm⁻¹ range, using a spectrometer equipped with a DTGS KBr (deuterated triglycine sulphate with potassium bromide windows) detector. A spectral resolution of 2 cm⁻¹ was chosen and each spectrum represented an average of 32 scans, corrected for the spectrum of the blank KBr pellet.

Optical images of the deposited CRL films were obtained by means of an Olympus microscope with 100× magnification, using a micrometric slide.

Atomic force microscopy (AFM) analysis was performed by means of a Nanoscope IIIa AFM (Veeco Instruments Inc., USA), operating in tapping mode (scan size and rate of 1 μm and 1 Hz, respectively), equipped with a silicon tip having nominal curvature radius of about 5 nm.

In order to assess the functionality of the deposited lipase, hydrolysis tests were performed by emulsifying 1 mL of soybean oil in 2 mL of distilled water by means of the surfactant tween 80® and magnetic stirring (500 rpm). After the emulsion was formed, the magnetic stirring was set at 200 rpm, the biocatalyst anchored to the solid support were immersed in the reaction mixture kept under stirring for 24 h. The reaction products were qualitatively characterized by reverse phase thin layer chromatography (RP-TLC), using precoated glass plates RP-18 and acetonitrile-ethylacetate 2.5:1 as mobile phase. 60 μL of each reacted mixture and of the untreated soybean oil were dissolved into 1 mL of dichloromethane and droplets of 2 μL of these solutions were deposited on the pencil spot on the bottom of the chromatographic plate. The plates were immersed for about 1 cm into the mobile phase and left for about fifteen minutes, then the solvent front was marked. The chromatographic plates were then dried at 150 °C on a hot plate. The chromatograms were detected by spraying H₂SO₄ 4 N on the dried chromatographic plates and heating them at 150 °C.

3. Results and discussion

Last column in Table 1 reports the laser pulse energy required to obtain a MAPLE film on the substrate. The addition of m-DOPA actually lowered the ablation threshold of the target thus allowing using a lower laser energy pulse. This behavior can be explained since around 1064 nm (the laser beam wavelength) there is the third overtone of C–H stretching of aromatic groups (catechol side chain of m-DOPA), while water does not have absorption bands near that wavelength: the presence of an even small amount of m-DOPA increased the overall laser energy absorption of the target.

To study film morphology in Fig. 1 we show the optical microscopy image of M-L2 (a) and M-L3 (b) samples. From Fig. 1(a) it can be appreciated the uniform coverage of the support. Nevertheless, the surface is

Table 1

Target composition and the corresponding pulsed laser energy required to obtain MAPLE deposition of the samples.

| Sample | Target composition | Laser pulse energy (mj/pulse) |
|--------|--|-------------------------------|
| M-L1 | Lipase (2%wt) in water | 526 |
| M-L2 | Lipase (1.8%wt) m-DOPA (0.2%wt) in water | 410 |
| M-L3 | Lipase (0.9%wt) m-DOPA (0.1%wt) in water | 410 |

very rough, showing micrometric clusters and crystalline inclusions that can be recognized by the regular shape (square or rectangular). From this micrograph it can be inferred that the starting solution was too concentrated to be able to get a good deposition, with lipase dispersed at or almost at molecular level. In order to improve film morphology, in sample M-L3 the concentration of both solutes was lowered, maintaining constant their ratio. The optical micrograph of the sample M-L3 showed in Fig. 1(b) displays the absence of micrometric features. The lipase film is not optically visible, but its presence is evidenced from its AFM (Atomic Force Microscope) image presented in Fig. 2 in a $2\ \mu\text{m} \times 2\ \mu\text{m}$ window.

From the AFM image a much smoother film appeared, with nanometric rather than micrometric features. The deposition of sample M-L3 resulted in nanofilms that provided a full coverage of the support.

The structural characteristics of the MAPLE deposited lipase were studied by means of FTIR spectroscopy. FTIR spectroscopy is widely used for studying the secondary structure of proteins [34–36]. Indeed different absorption bands arising from the protein backbone depends on the structural context (α -helices, β -sheets, turns) of the bond involved in the vibration. Among these, of particular utility is the band designated as Amide I between 1600 and $1700\ \text{cm}^{-1}$, which originates primarily from the stretching vibrations of the $\text{C}=\text{O}$ bond. This band is due to the overlapping of different modes depending of the nature of hydrogen bonding $\text{C}=\text{O}\cdots\text{H}-\text{N}$, determined by the secondary structure of the protein. In details, three main secondary structure elements can be observed at 1650 – $1660\ \text{cm}^{-1}$ (α -helices), 1620 – $1650\ \text{cm}^{-1}$ (β -sheets) and 1660 – $1690\ \text{cm}^{-1}$ (turns and other disordered structures). At lower wavenumbers, 1610 – $1620\ \text{cm}^{-1}$, absorption is attributed to strongly intermolecular hydrogen-bonded β -sheets structures [37].

Quantitative analysis of the protein secondary structure was performed by assuming that the amide I band was the linear combination of Gaussian components arising from the various secondary structure elements. The number and initial positions of these components were set from the second derivative spectra, obtained after a binomial 5 point smoothing of the spectra (Savitzky–Golay method). Curve fitting was then performed using a fixed bandwidth ($12\ \text{cm}^{-1}$) and a Gaussian profile. The intensity of each component was determined by the best fit results.

The FTIR spectra of the three samples in the region 1525 – $1775\ \text{cm}^{-1}$, together with the amide I curve fitting into its Gaussian component, are shown in Fig. 3. As can be seen, the peak representing aggregated β -strands, i.e. stretching vibrations of intermolecular H-bonded $\text{C}=\text{O}$ in self-association at 1610 – $1620\ \text{cm}^{-1}$, lose progressively intensity by going from M-L1 to M-L3 in favor of the intensity of the peaks representing native secondary structure elements.

Each component was correlated with the amount of peptide bonds in the structural unit from which the component originated, by dividing the area under each component by the total area [38]. Quantitative results of the curve fitting procedure for the three samples under study and Gaussian component attribution are reported in Table 2. Peaks before $1600\ \text{cm}^{-1}$ and after $1700\ \text{cm}^{-1}$ are attributed to the side-chains vibrations [38,34] and are not included in the calculation. In particular, the Gaussian peak appearing after the deconvolution at $1585\ \text{cm}^{-1}$ is due to COO^- antisymmetric stretching of Asp and Glu carboxylate groups [38].

From the data in Table 2 it can be inferred that the sample deposited without the addition of m-DOPA (M-L1) showed a high degree of unfolding/aggregation/self-association ($1624\ \text{cm}^{-1}$) of lipase molecules, especially at the expense of the secondary structure elements β -sheets and turns. In fact, in the native conformation of *Candida Rugosa* Lipase α -helices accounts for about 40%, while β -sheets for 23%, and turns for 28% as predicted by FTIR [40]. Adding m-DOPA reduced the percentage of self-association. Decreasing the concentration of the solute in the target (sample M-L3) further reduced the unfolding/aggregation occurring during the MAPLE process and the α -helices proportion almost reached that of the native conformation indicating that aggregation mainly occurred at the expenses of β -sheets. However some degree of unfolding/aggregation was still present in M-L3 sample, as indicated in Table 2.

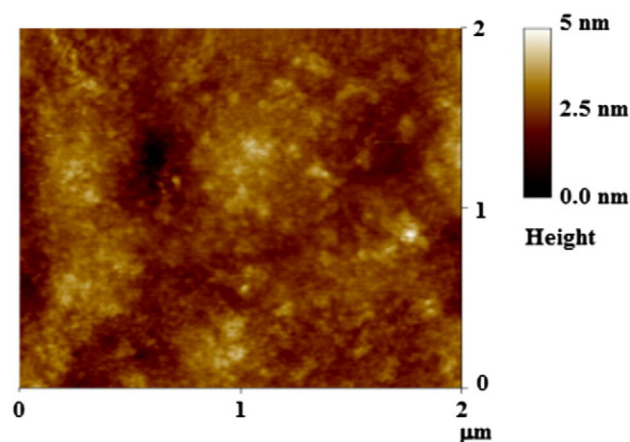


Fig. 2. $2\ \mu\text{m} \times 2\ \mu\text{m}$ AFM image of sample M-L3.

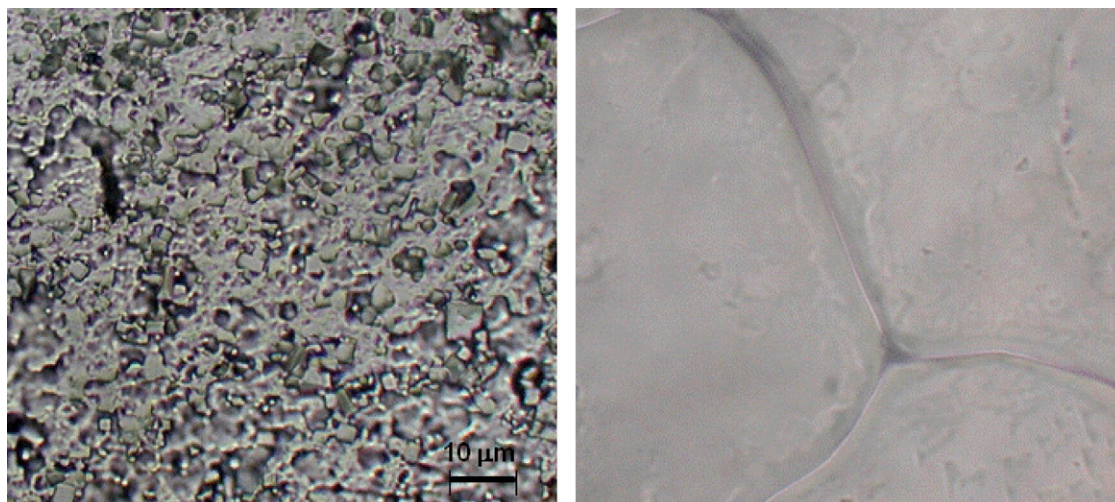


Fig. 1. Optical image of samples (a) M-L2 and (b) M-L3.

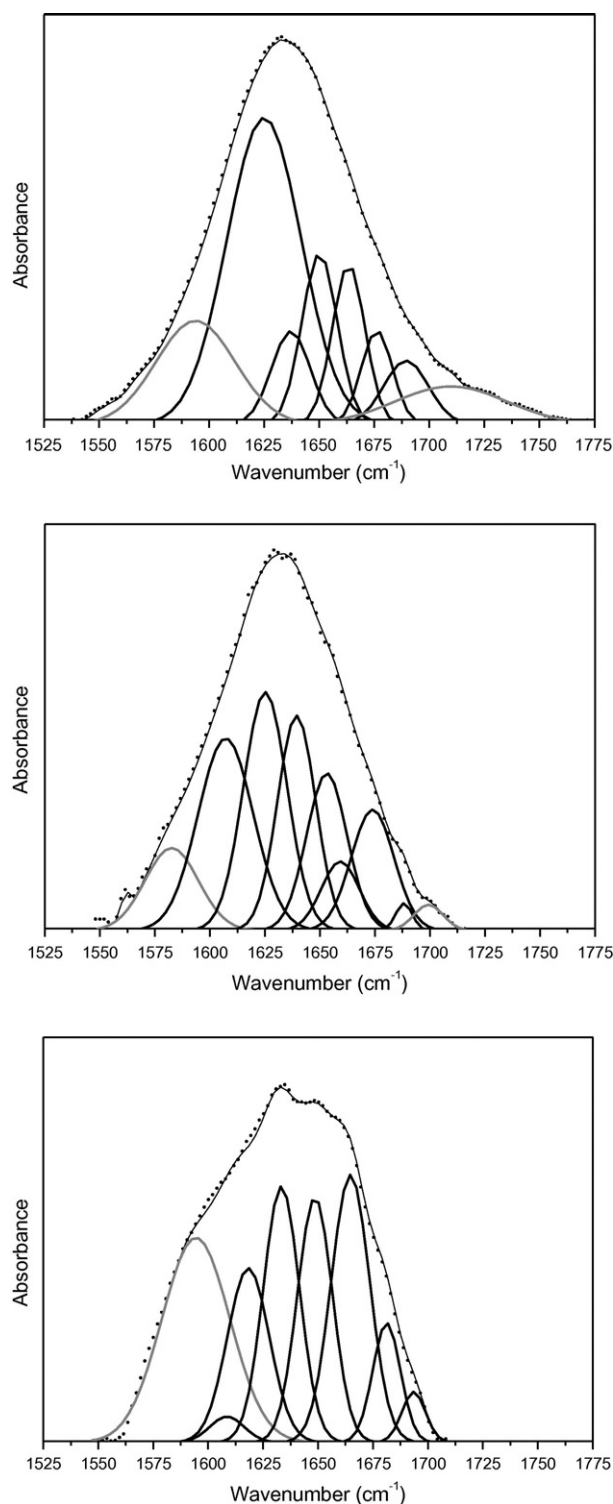


Fig. 3. FTIR spectra and deconvolution into Gaussian components: — curve fitted spectra; ● measured absorption spectra. Top: M-L1 [25], middle M-L2, bottom M-L3.

The above analysis is also confirmed by the behavior of the amide A band around 3300 cm^{-1} , illustrated in Fig. 3 for the three samples under study, compared with that of the unprocessed lyophilized lipase (pressed into a KBr pellet). This band is due to the stretching of the N–H bond. It is exclusively localized on the NH group and is therefore insensitive to the conformation of the polypeptide backbone. However, the frequency of the amide A vibration depends on the strength of the hydrogen bond [34]. In particular, N–H bonds in α -helices and β -sheets absorb around 3300 cm^{-1} , while in random-coil structure the

Table 2
Position and percentage area of the Gaussian component deriving from the best fit of FTIR spectra of samples ML1, ML2 and ML3.

| Gaussian component position (cm^{-1}) | | | % Area | | | Attribution |
|--|------|------|--------|------|------|--|
| ML1 | ML2 | ML3 | ML1 | ML2 | ML3 | |
| 1624 | 1607 | 1618 | 55.4 | 47.1 | 27.1 | Intermolecular H-bonded CO in self-association [38–40] |
| | 1625 | | | | | |
| 1637 | 1639 | 1633 | 7.71 | 18.3 | 16.9 | H-bonded CO in β -sheets [34] |
| 1650 | 1653 | 1648 | 23.0 | 20.3 | 38.5 | H-bonded CO in α -helices [34] |
| 1663 | 1659 | 1665 | | | | |
| 1676 | 1673 | 1681 | 13.8 | 14.3 | 17.5 | Turns [38] |
| 1693 | 1688 | 1693 | | | | |
| | 1699 | | | | | |

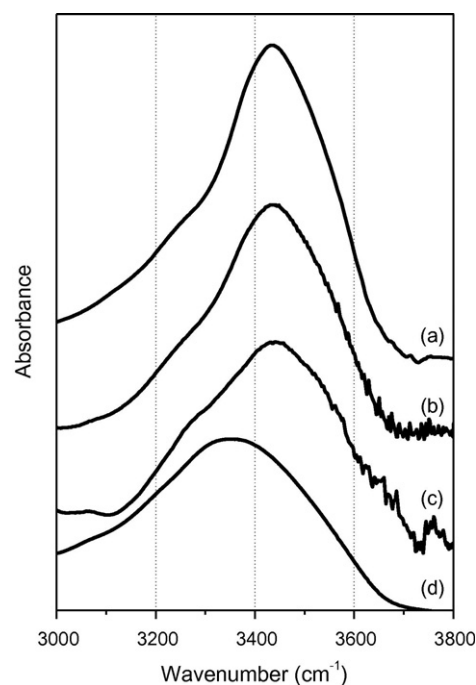


Fig. 4. FTIR spectra of samples (a) M-L1, (b) M-L2, (c) M-L3 and (d) unprocessed lipase in the amide A absorption region.

absorption band shifts towards 3400 cm^{-1} due to the rupture of the H-bonds [41]. Going from ML1 to ML3, a component at 3440 cm^{-1} representing H-unbound random coil structures progressively loses intensity, while that at 3300 cm^{-1} increases, substantiating the decreasing degree of unfolding in ML2 and ML3.

This trend outlined the efficacy of m-DOPA in protecting lipase during the MAPLE process. One reason for this is by acting as a radiation absorber, lowering the laser energy required for the deposition. Furthermore, thanks to the two hydroxyl groups of the catechol side chain, m-DOPA provided hydrogen bonds with the polypeptide that can protect lipase from denaturing [42], helping to preserve its native form, both during the freezing phase of the MAPLE process and during the dehydration phase occurring in the target-to-substrate journey. In fact it was found that the addition of hydrogen bonding donor amino acids exerted a protective effect on protein secondary structure upon freeze-drying in a concentration-dependent manner [31]. The stabilization was supposed to proceed via the water replacement hypothesis, a mechanism which involves the formation of hydrogen bonds between a protein and an excipient at the end of the drying process that satisfy hydrogen bonding requirements of polar groups on the surface of the polypeptide. The excipient concentration was higher than the one utilized in this work (15–71% w/w vs. 10% w/w) and the efficacy of the

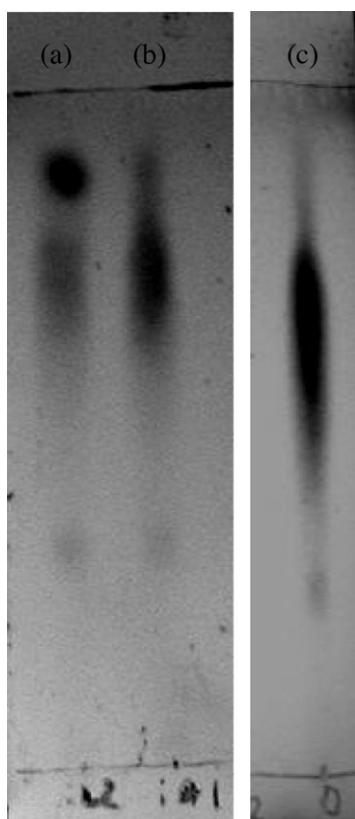


Fig. 5. TLC of soybean oil using as catalyst (a) 15 mg of free-CRL, (b) MAPLE deposited lipase, sample M-L2 and (c) unreacted soybean oil.

addition increased with concentration. This opens the possibility of increasing m-DOPA concentration in order to obtain a better protective effect on the secondary structure of lipase.

Preliminary catalytic essays were carried out using as biocatalyst the sample M-L2 in the hydrolysis of soybean oil. Reaction products were qualitatively characterized by reverse RP-TLC comparing the results to those obtained using as biocatalyst 15 mg of CRL lyophilized powder. The chromatograms are shown in Fig. 5. For comparison, the chromatogram of untreated soybean oil is also reported.

Reverse phase separation enabled the resolution of the reacted mixture into triglycerides (TGs), diglycerides (DGs), monoglycerides (MGs) and free fatty acids (FFA). The order of retention on the chromatographic layer of the sample components follows the adsorption/partition type mechanisms. The MGs, being the more polar, exhibit the least retention and hence migrate up towards the solvent front followed by the FFA, DGs and finally TGs [43].

The chromatogram of Fig. 4(a) and (b) showed the residual oil spots below that of the hydrolysis products that, being more polar, were less retained by apolar stationary phase. Furthermore, in the chromatogram of Fig. 4(b), there is a halo that traveled farther the FFA and that is due to MGs reaction intermediates. The chromatogram of the oil in Fig. 4(c), on the other hand, was much more elongated in the TG region and did not show a neat spot representing the fatty acids. The oil chromatogram appears elongated due to the variation in saturation and chain length of the component fatty acids [43]. Instead the stain left behind the TGs spot is due to some apolar compound present in the soybean oil and its appearance does not depend on the reaction, since it is always present both in the oil and in the reacted mixtures. By observing the different areas and intensity of the burnt spot representing the fatty acids, and considering the presence of MGs reaction intermediates in the chromatogram of the reaction catalyzed by M-L3, it is evident that the reaction catalyzed by the MAPLE sample occurred to a smaller degree. Nevertheless it did occur, and the smaller quantity of fatty acids

obtained could depend on the smaller quantity of catalyst used (about 1 mg after MAPLE deposition).

4. Conclusions

Lipase, a catalyst in the hydrolysis of triacylglycerol to glycerol and fatty acids, is used in biosensors for detection of triglycerides in blood serum. A key issue is its deposition/immobilization on a substrate. In a previous paper, we introduced the use of MAPLE technique to deposit lipase, showing that the whole process (target freezing, laser irradiation, impact on the substrate and vacuum exposition) can be carried out partially preserving the enzyme activity. Here we suggest that the addition of a small amount of m-DOPA can protect lipase from denaturation induced by freezing of the target and by drying during its travel in the vacuum towards the substrate. Further studies are being carried out, but these preliminary results lead us to the novel results that the presence of m-DOPA in the deposition mixture reduces the required laser energy in about 20% for the MAPLE deposition and, as far as we can see today, it does not chemically affect the enzymatic activity of lipase. Moreover its chemical features should improve adhesion and therefore give a better immobilization of lipase.

References

- [1] R. Eason (Ed.), *Pulsed Laser Deposition of Thin Films*, John Wiley & Sons, New York, NY, USA, 2007 ISBN: 987-0-471-44709-2.
- [2] D.B. Chrisey, A. Pique, R.A. McGill, J.S. Horwitz, B.R. Ringeisen, D.M. Bubb, P.K. Wu, *Chem. Rev.* 103 (2003) 553–576, <http://dx.doi.org/10.1021/cr010428w>.
- [3] A. Pique, R.A. McGill, D.B. Chrisey, D. Leonhardt, T.E. Mslin, B.J. Spargo, J.H. Callahan, R.W. Vachet, R. Chung, M.A. Bucaro, *Thin Solid Films* 355–356 (1999) 536–541, [http://dx.doi.org/10.1016/S0257-8972\(99\)00376-X](http://dx.doi.org/10.1016/S0257-8972(99)00376-X).
- [4] F. Bloisi, M. Barra, A. Cassinese, L.R.M. Vicari, *J. Nanomaterials* (2012) 9, <http://dx.doi.org/10.1155/2012/395436> Article ID 395436.
- [5] Valeria Califano, Francesco Bloisi, Antonio Aronne, Stefania Federici, Libera Nasti, Laura E. Depero, Luciano R.M. Vicari, *Biosensors* 4 (2014) 329–339, <http://dx.doi.org/10.3390/bios4040329>.
- [6] R. Fryčeka, M. Jelínek, T. Kocourek, P. Fitl, M. Vřníta, V. Myslík, M. Vrbová, *Thin Solid Films* 495 (2006) 308–311, <http://dx.doi.org/10.1016/j.tsf.2005.08.178>.
- [7] E.J. Houser, D.B. Chrisey, M. Bercu, N.D. Scarisoreanu, A. Purice, D. Colceag, C. Constantinescu, A. Moldovan, M. Dinescu, *Appl. Surf. Sci.* 252 (2006) 4871–4876, <http://dx.doi.org/10.1016/j.apsusc.2005.07.159>.
- [8] F. Bloisi, L. Vicari, R. Papa, V. Califano, R. Pedrazzani, E. Bontempi, L.E. Depero, *Mater. Sci. Eng. C* 27 (2007) 1185–1190, <http://dx.doi.org/10.1016/j.msec.2006.12.005>.
- [9] A.P. Caricato, M. Lomascolo, A. Luches, F. Mandoj, M.G. Manera, M. Mastroianni, M. Martino, R. Paolesse, R. Rella, F. Romano, T. Tunno, D. Valerini, *Appl. Phys. A* 93 (2008) 651–654, <http://dx.doi.org/10.1007/s00339-008-4724-7>.
- [10] V. Califano, F. Bloisi, L.R.M. Vicari, O. Bretcanu, A.R. Boccaccini, *J. Biomed. Opt.* 13 (2008) <http://dx.doi.org/10.1117/1.2830660> Article ID 014028.
- [11] R. Cristescu, D. Mihaiescu, G. Socol, I. Stamatin, I.N. Mihaiescu, D.B. Chrisey, *Appl. Phys. A* 79 (2004) 1023–1026, <http://dx.doi.org/10.1007/s00339-004-2619-9>.
- [12] I. Stamatin, R. Cristescu, G. Socol, A. Moldovan, D. Mihaiescu, I. Stamatin, I.N. Mihaiescu, D.B. Chrisey, *Appl. Surf. Sci.* 248 (2005) 422–427, <http://dx.doi.org/10.1016/j.apsusc.2005.03.060>.
- [13] B.R. Ringeisen, J. Callahan, P.K. Wu, A. Piqué, B. Spargo, R.A. McGill, M. Bucaro, H. Kim, D.M. Bubb, D.B. Chrisey, *Langmuir* 17 (2001) 3472–3479, <http://dx.doi.org/10.1021/la0016874>.
- [14] A. Purice, J. Schou, P. Kingshott, N. Pryds, M. Dinescu, *Appl. Surf. Sci.* 253 (2007) 6451–6455, <http://dx.doi.org/10.1016/j.apsusc.2007.01.066>.
- [15] M. Trojanowicz, *Electrochem. Commun.* 38 (2014) 47–52, <http://dx.doi.org/10.1016/j.elecom.2013.10.034>.
- [16] M. Cardosi, B. Haggert, in: M. Campbell (Ed.) *Biosensor Devices*. In *Sensor Systems for Environmental Monitoring* Chapman & Hall, London, UK, 1997 <http://dx.doi.org/10.1007/978-94-009-1571-8-7> ISBN: 978-94-010-7202-1.
- [17] R.H. Eckel, *Lipoprotein lipase*, *N. Engl. J. Med.* 320 (1989) 1060–1068.
- [18] T. Kullick, R. Ulber, H.H. Meyer, T. Scheper, K. Schugerl, *Anal. Chim. Acta* 293 (271–27) (1994) 6, [http://dx.doi.org/10.1016/0003-2670\(94\)85032-1](http://dx.doi.org/10.1016/0003-2670(94)85032-1).
- [19] M.S. Veeramani, K.P. Shyam, N.P. Ratchagar, A. Chadha, B. Bhattacharya, *Anal. Methods* 6 (1728–173) (2014) 5, <http://dx.doi.org/10.1039/C3AY42274G>.
- [20] M. Nasratun, H.A. Said, A. Noraziah, A.N.A. Alla, *Am. J. Appl. Sci.* 6 (2009) 1653–1657, <http://dx.doi.org/10.3844/ajassp.2009.1653.1657>.
- [21] D. Pirozzi, E. Fanelli, A. Aronne, P. Pernice, A. Mingione, *J. Mol. Catal. B: Enzym.* 59 (2009) 116–120, <http://dx.doi.org/10.1016/j.molcatb.2009.01.010>.
- [22] D.H. Lee, C.H. Park, J.M. Yeo, S.W. Kim, *J. Ind. Eng. Chem.* 12 (2006) 777–782.
- [23] U.H. Zaidan, M.B.A. Rahman, S.S. Othman, M. Basri, E. Abdulmalek, R.N.Z.R.A. Rahman, A.B. Salleh, *Food Chem.* 131 (2012) 199–205.
- [24] Z.D. Knežević, S.S. Šiler-Marinković, L.V. Mojović, *APTEFF* 35 (2004) 1–280.
- [25] A. Aronne, G. Ausanio, F. Bloisi, R. Calabria, V. Califano, E. Fanelli, P. Massoli, L.R.M. Vicari, *Appl. Surf. Sci.* 320 (2014) 524–530, <http://dx.doi.org/10.1016/j.apsusc.2014.09.112> ISSN: 0169-4332.

- [26] J.L. Dalsin, P.B. Messersmith, *Mater. Today* 8 (2005) 38.
- [27] T. Deming, *J. Curr. Opin. Chem. Biol.* 3 (1999) 100.
- [28] J.L. Dalsin, B.H. Hu, B.P. Lee, P.B. Messersmith, *J. Am. Chem. Soc.* 125 (2003) 4253.
- [29] A. Doraiswamy, R.J. NaraYan, R. Cristescu, I.N. Mihailescu, D.B. Chrisey, *Mater. Sci. Eng. C* 27 (2007) 409.
- [30] V. Califano, F. Bloisi, L.R.M. Vicari, Paolo Colombi, Elza Bontempi, Laura E. Depero, *Appl. Surf. Sci.* 254 (2008) 7143–7148.
- [31] Fei Tian, C. Russell Middaugh, Tom Offerdahl, Eric Munson, Samir Sane, J. Howard Rytting, *Int. J. Pharm.* 335 (2007) 20–31.
- [32] Bo Stenberg, Raphael A. Viscarra Rossel, Abdul Mounem Mouazen, Johanna Wetterlind, *Visible and Near Infrared Spectroscopy in Soil Science*, in: Donald L. Sparks (Ed.) *Advances in Agronomy*, 107, Academic Press, Burlington 2010, pp. 163–215, [http://dx.doi.org/10.1016/S0065-2113\(10\)07005-7](http://dx.doi.org/10.1016/S0065-2113(10)07005-7).
- [33] M.L. Foresti, M.L. Ferreira, *Anal. Bioanal. Chem.* 381 (2005) 1408–1425.
- [34] Andreas Barth, *Infrared spectroscopy of proteins*, *Biochim. Biophys. Acta* 1767 (2007) 1073–1101.
- [35] J. Kong, S. Yu, *Fourier transform infrared spectroscopic analysis of protein secondary structure*, *Acta Biochim. Biophys. Sin (Shanghai)* 39 (2007) 549–559.
- [36] J.L.R. Arrondo, A. Muga, J. Castresana, F.M. Goni, *Quantitative studies of the structure of proteins in solution by fourier-transform infrared spectroscopy*, *Prog. Biophys. Mol. Biol.* 59 (1993).
- [37] Z. Zhou, A. Inayat, W. Schwieger, M. Hartmann, *Improved activity and stability of lipase immobilized in cage-like large pore mesoporous organosilicas*, *Microporous Mesoporous Mater.* 154 (2012) 133–141.
- [38] S. Noinville, M. Revault, M. Baron, A. Tiss, S. Yapoudjian, M. Ivanova, R. Verger, *Conformational changes and orientation of Humicola lanuginosa lipase on a solid hydrophobic surface: an in Situ interface Fourier transform infrared-attenuated total reflection study*, *Biophys. J.* 82 (2002) 2709–2719.
- [39] S.E. Collins, V. Lassalle, M.J. Ferreira, *FTIR-ATR characterization of free Rhizomucor meihei lipase (RML), Lipozyme RM IM and chitosan-immobilized RML*, *J. Mol. Catal. B: Enzym.* 72 (2011) 220–228.
- [40] A. Natalello, D. Ami, S. Brocca, M. Lotti, S.M. Doglia, *Secondary structure, conformational stability and glycosylation of a recombinant Candida rugosa lipase studied by Fourier-transform infrared spectroscopy*, *Biochem. J.* 385 (2005) 511–517.
- [41] P. Narayanan, *Essential of Biophysics*, New Age International Ed, New Delhi, 2000 p. 219.
- [42] P.O. Souillac, C.R. Middaugh, J.H. Rytting, *Investigation of protein/carbohydrate interactions in the dried state. 2. Diffuse reflectance FTIR studies*, *Int. J. Pharm.* 235 (2002) 207–218.
- [43] P.E. Wall III, *Triglycerides Thin-Layer (Planar) Chromatography*, in: M. Wilson, C.F. Cooke (Eds.), *Encyclopedia of Separation Science* Academic Press, London 2000, pp. 4412–4420.